

Interaction between multi-component vortices at arbitrary distances using a variational method in the Ginzburg–Landau theory

Hadi Lookzadeh^a, Sedigheh Deldar^b

Department of Physics, University of Tehran, Tehran, Iran

Received: 17 August 2014 / Accepted: 20 September 2014 / Published online: 15 October 2014
© The Author(s) 2014. This article is published with open access at Springerlink.com

Abstract We study the interaction between the vortices in multi-component superconductors based on the Jacobs and Rebbi variation method using Ginzburg–Landau theory. With one condensation, we get attraction interaction between the vortices for type I and repulsion for type II superconductors. With two condensation states such as MgB_2 superconductors the behavior is quite different. There is attraction at large distances and repulsion when the vortices are close to each other. A stability point at distance $2.7/\lambda_1$ is obtained. In the case of three condensation states such as iron based superconductors, we see different behavior depending on penetration depth and correlation length. The formation energy of a vortex with three condensation states is larger than the one with one condensation state with comparable penetration and correlation length. We obtain two stability points for the superconductors with three condensation states.

1 Introduction

The interaction between the elementary particles can be described by means of a field of force, just as the interaction between the charged particles which is described by the electromagnetic field. In quantum field theory, the electromagnetic field is accompanied by photon. Attraction and repulsion of electric charged particles can be described by exchanging particles called virtual photons [1]. On the other hand topological defects are also important structures in physics since they can affect the properties of matter or even the phase structure of a system. These structures, such as vortices, monopoles, strings, and instantons, can interact with each other like particles. They even have interaction with particles [2]. In this paper we study the interaction between the

vortices in superconductor materials based on a variational numeric computation for arbitrary separation between the vortices [3–5]. This method is useful in some phenomenological models. Vortices are solutions of the Ginzburg–Landau equations [6, 7]. These equations give a topological structure with finite energy. The Ginzburg–Landau equations are at least two nonlinear coupled equations, so there is no exact analytical solution for these equations. As the order of the nonlinearity is not small, it is not possible to use the usual perturbation methods to study the G-L Lagrangian behavior. Nevertheless, it is possible to study their behavior at asymptotic distances. Knowing the asymptotic behaviors of the functions, we can have an ansatz for these solutions for any arbitrary distances [5].

For the first time Abrikosov predicted the existence of a vortex structure in superconductors [8–11]. He suggested that the form of magnetic field penetration in a superconductor can be described by vortex equations. He studied the vortex properties by a Ginzburg–Landau theory. The G-L Lagrangian looks like an Abelian Higgs model where the Higgs field is like the order parameter and the gauge field is the electromagnetic field. The normal core of the vortex is introduced by the superconductor correlation length ξ and the London penetration depth λ . There are two types of superconductors [12, 13] depending on the Ginzburg–Landau parameter $\kappa = \lambda/\xi$. For $\kappa < 1/\sqrt{2}$, the magnetic penetration depth is smaller than the correlation length. This is the type I superconductor, for which the vortex structure is not stable. The interaction between vortices of this type is attraction. For $\kappa > 1/\sqrt{2}$, the magnetic penetration depth is larger than the correlation length, this is type II superconductor. The magnetic field can penetrate in these materials. The vortex structure is stable. There is repulsion between these vortices and they form a triangular vortex lattice [12, 13]. For $\kappa = 1/\sqrt{2}$, called the Bogomol’nyi point or type I/II border, there is no interaction between the vortices.

^a e-mail: h.lookzadeh@ut.ac.ir

^b e-mail: sdeldar@ut.ac.ir

Depending on the distance between the vortices, various methods can be chosen to study the interaction between them. Kramer [4] used asymptotic behavior of a vortex fields to obtain an analytical expression for the vortex–vortex interaction energy when they are far from each other. The fields can be explained by modified Bessel functions at the asymptotic regime; but what about the vortex interaction when they are close to each other? Jacobs and Rebbi used a variation method to obtain approximate trial functions describing the fields of two vortices at arbitrary distances [5]. Variational parameters were obtained by minimizing the free energy. Their method can predict the results of Kramer for large distances. It also predicts the same type of interaction for the small distances in type I and type II superconductors. There are other methods to study the interaction between the vortices [14–20].

A superconductor with more than one condensation state is called a multi-band superconductor. MgB_2 and iron pnictide superconductors are of this type. These materials have a higher phase transition temperature with respect to the usual superconductors of type I and II. They behave differently compared with the type I or type II superconductors with one condensation state. Also the possibility of the existence of more than three condensation states has been recently studied from the theoretical point of view [21]. Interaction between these vortices is different from the usual superconductors [22–30]. Babaev and Speight have studied theoretically [31, 32] what happens when the value of magnetic penetration depth is between two condensation lengths; vortices may attract each other at large separations and repel each other at short distances. This kind of superconductor, called type 1.5 in the literature, is type I corresponding to one of its condensation and type II with respect to the other one.

In this paper we use a G-L Lagrangian and the variational method of Jacobs and Rebbi to study the interaction between the vortices with three condensation states. The G-L theory is valid near the critical temperature. A different coordinate system, the polar coordinate system, is used in our calculations. Since a single vortex has a circular symmetry or $SO(2)$ symmetry, choosing a polar coordinate system simplifies the calculations [3]. However, when we have two vortices in a plane, we lose this symmetry and only a reflection symmetry with respect to the plane remains. The plane is located between the vortices. First we use this method for a vortex with one condensation. Then we apply it for two and three condensations. The case with three condensations is different from the one with two condensations. The energy of formation of vortices of type 1.5 is larger than the energy of type I and type II. Since the materials with multi-band condensation states are high temperature superconductors, the formation of these nonlinear structures with higher energy than usual superconductors may have some relations with the higher critical temperature in this kind of superconductors. Using

this method of calculation one can suggest the values of the correlation lengths and penetration depths which increase the current known phase transition temperatures.

2 The Ginzburg–Landau theory for multi-band component superconductor

The free energy of G-L theory can be given by

$$E = \int \mathcal{F} d\mathbf{r}, \quad (1)$$

where the functional \mathcal{F} is

$$\mathcal{F} = \alpha |\Psi|^2 + \frac{\beta}{2} |\Psi|^4 + \frac{1}{2m} \left| \left(-i\hbar\nabla - \frac{2e}{c} \mathbf{A} \right) \Psi \right|^2 + \frac{1}{8\pi} (\nabla \times \mathbf{A})^2, \quad (2)$$

the complex scalar field ψ is the order parameter or the condensation state. \mathbf{A} is a vector potential for magnetic field. α and β are the parameters that can be determined phenomenologically from the correlation length $\xi = \hbar/\sqrt{4m\alpha}$ and the penetration depth $\lambda = \sqrt{mc^2\beta/8\pi|\alpha|c^2}$ of the superconducting matter [7]. α is a temperature dependent parameter and is defined as $\alpha(T) = \alpha(0)(1 - T/T_c)$ with $\alpha(0) < 0$.

One can generalize Eq. (2) to a multi-band superconductor by increasing the number of condensation states. For example for two bands, the G-L theory can be introduced with two order parameters $|\psi|$ and for three bands with three states. In the G-L theory one may consider other contributions up to ψ^4 terms. The contributions of all types of possible interactions between fields in the G-L theory should be considered including $\psi_i\psi_j$, called interband coupling, $|\psi_i|^2|\psi_j|^2$ etc. The interband coupling terms, which do not exist in the usual superconductor, imply some new properties for the type 1.5 superconductors. For the present work we consider only the interband coupling terms. The free energy functional for two condensation states is

$$\mathcal{F} = \sum_{i=1,2} \left[\alpha_i |\Psi_i|^2 + \frac{\beta_i}{2} |\Psi_i|^4 + \frac{1}{2m_i} \left| \left(-i\hbar\nabla - \frac{2e}{c} \mathbf{A} \right) \Psi_i \right|^2 \right] + \frac{1}{8\pi} (\nabla \times \mathbf{A})^2 - \gamma (\Psi_1^* \Psi_2 + \Psi_2^* \Psi_1), \quad (3)$$

where $\gamma(T) = \gamma(0)(1 - T/T_c)$ (and $\gamma(0) = -0.4\alpha(0)$) is the condensations coupling. The free energy functional for the case with three condensations is

$$\begin{aligned} \mathcal{F} = & \sum_{i=1,2,3} \left[\alpha_i |\Psi_i|^2 + \frac{\beta_i}{2} |\Psi_i|^4 \right. \\ & + \frac{1}{2m_i} \left| \left(-i\hbar\nabla - \frac{2e}{c} \mathbf{A} \right) \Psi_i \right|^2 \Big] \\ & + \frac{1}{8\pi} (\nabla \times \mathbf{A})^2 - \gamma_1 (\Psi_1^* \Psi_2 + \Psi_2^* \Psi_1) \\ & - \gamma_2 (\Psi_2^* \Psi_3 + \Psi_3^* \Psi_2) - \gamma_3 (\Psi_1^* \Psi_3 + \Psi_3^* \Psi_1). \end{aligned} \tag{4}$$

For convenience we use the dimensionless quantities

$$\begin{aligned} x = \lambda_1 x', \quad \Psi_i = \Psi_{10} \Psi'_i, \quad \mathbf{A} = \lambda_1 H_{1c} \sqrt{2} \mathbf{A}', \\ \mathcal{F} = \frac{H_{1c}^2}{4\pi} \mathcal{F}', \tag{5} \\ \gamma = \gamma' |\alpha_1|, \quad \mathbf{B} = H_{1c} \sqrt{2} \mathbf{B}', \quad \mathbf{J} = \frac{2e\hbar\Psi_{10}^2}{m_1\xi_1} \mathbf{J}', \end{aligned}$$

$\psi_{10}^2 = |\alpha_1|/\beta_1$ is called the bulk value and $H_{1c} = \sqrt{4\pi\alpha_1\psi_{10}^2}$ is the thermodynamic critical field of the first condensate. \mathbf{B} is the magnetic field and \mathbf{J} is the super current. Omitting the prime for the dimensionless quantities, we have

$$\begin{aligned} \mathcal{F} = & \sum_{i=1,2,3} \left[\frac{\alpha_i}{|\alpha_1|} |\Psi_i|^2 + \frac{\beta_i}{2\beta_1} |\Psi_i|^4 \right. \\ & + \frac{m_1}{m_i} \left| \left(\frac{1}{i\kappa_1} \nabla - \mathbf{A} \right) \Psi_i \right|^2 \Big] \\ & + (\nabla \times \mathbf{A})^2 - \gamma_1 (\Psi_1^* \Psi_2 + \Psi_2^* \Psi_1) \\ & - \gamma_2 (\Psi_2^* \Psi_3 + \Psi_3^* \Psi_2) - \gamma_3 (\Psi_1^* \Psi_3 + \Psi_3^* \Psi_1). \end{aligned} \tag{6}$$

The Euler–Lagrange equations can be obtained by

$$\begin{aligned} \frac{\partial \mathcal{F}}{\partial \Psi_\alpha} - \sum_i \frac{\partial}{\partial x_i} \frac{\partial \mathcal{F}}{\partial (\partial \Psi_\alpha / \partial x_i)} = 0, \\ \frac{\partial \mathcal{F}}{\partial A_i} - \sum_i \frac{\partial}{\partial x_i} \frac{\partial \mathcal{F}}{\partial (\partial A_i / \partial x_i)} = 0. \end{aligned} \tag{7}$$

Solving these equations is not straightforward. One can use a finite difference technique and a relaxation method suitable for nonlinear coupled differential equations to obtain the solutions which are used by Peeters [14–20]. Also it is possible to discretize the space and time with a method of lattice gauge theory to obtain the solutions [13]. However, in this paper we use the variational method introduced by Jacobs and Rebbi to obtain trial functions for condensations and the vector potential. The advantage is that we can work analytically with these variational functions. However, it is a long analytical calculation. This method may be useful for studying the interaction between the vortices in the phenomenological models of particle physics which study the confinement problem [33–38].

3 Interaction between the vortices in type I and type II superconductors

We use the dimensionless free energy functional of (2). Then the G-L equations from (7) are obtained:

$$-\Psi + |\Psi|^2 \Psi + \left(\frac{1}{i\kappa} \nabla - \mathbf{A} \right)^2 \Psi = 0, \tag{8}$$

$$\nabla \times \nabla \times \mathbf{A} = \frac{1}{2i\kappa_1} (\Psi^* \nabla \Psi - \Psi \nabla \Psi^*) - |\Psi|^2 \mathbf{A}, \tag{9}$$

where $\kappa_1 = \lambda_1/\xi_1$. In Ref. [5] a solution (ansatz) for ψ and \mathbf{A} for the above equations is suggested:

$$\Psi = f(r) e^{in\theta} \quad \text{and} \quad \mathbf{A} = \frac{na(r)}{\kappa_1 r} \mathbf{e}_\theta. \tag{10}$$

These are true for a straight vortex line type structure along the axis z . r is the distance from the center of the vortex core. \mathbf{e}_θ is the unit vector, θ is the azimuthal direction, and n represents the vorticity or the winding number. It is natural to discuss these circularly symmetric solutions in polar coordinates. Thus the fields are $\Psi(r, \theta)$, $A_r(r, \theta)$, and $A_\theta(r, \theta)$. We shall use the circular and reflection symmetries to obtain a reduced GL energy function, an integral just over the radial coordinate r . The variational equations are the reduced field equations. By the principle of symmetric criticality described in [3], solutions of these reduced equations give solutions of the full field equations in the plane. Substituting (10) in (8) and (9),

$$\begin{aligned} -f(r) + f^3(r) - \frac{1}{\kappa_1^2} \left(\partial_r^2 f + \frac{1}{r} \partial_r f \right) \\ + \frac{n^2(a-1)^2}{\kappa_1^2 r^2} f = 0, \end{aligned} \tag{11}$$

$$\partial_r^2 a - \frac{1}{r} \partial_r a + (f^2)(1-a) = 0. \tag{12}$$

The asymptotic forms of f and a for these explicit expressions do exist. We define the functions F and G such that

$$f(r) = 1 + F(r), \quad a(r) = 1 + G(r) \tag{13}$$

where F and G are small at large r . Thus substituting (13) in (11) and (12) and linearizing with respect to F and G one would get modified Bessel’s equations of zeroth order for F as a function of $k_1 r$ and first order for G/r as a function of r , respectively. Hence for $r \gg 1$

$$F \approx K_0(\sqrt{2}k_1 r), \quad G \approx r K_1(r), \tag{14}$$

where K_n is the n th modified Bessel’s function of the second kind (note that $K_1 = -K'_0$). Solutions exist for any $N \neq 0$ and can be found numerically. Near $r = 0$, $f(r) \approx r^N$. From the above equations, the asymptotic values of f and a , f_0 and a_0 , for $r \rightarrow \infty$ are obtained:

$$-1 + f_0^2 = 0, \quad a_0 = 1. \tag{15}$$

The radial variation of the wave functions and vector potential in the asymptotic region of $r \rightarrow \infty$ can be found and are given by

$$f(r) = 1 + c_{f_1} \exp\left(-\frac{r}{\sqrt{2}\xi}\right), \tag{16}$$

$$a(r) = 1 + c_a \exp\left(-\frac{r}{\lambda}\right), \tag{17}$$

where c_{f_1} and c_a are the coefficients that can be found. Nielsen and Olesen [8–11] obtained similar solutions at the asymptotic region. These are also called Nielsen–Olesen solutions. Having the asymptotic behavior of the solutions at $r = 0$ and $r \rightarrow \infty$ one would suggest acceptable fitting functions that would recover these asymptotic, and can give acceptable intermediate behavior. A polynomial times an exponential would be a good solution. The coefficients of the polynomial must be obtained numerically. Jacobs and Rebbi used a variational method to obtain these coefficients. To obtain $f(r)$, variational functions are suggested [5] and the asymptotic behaviors of $f(r)$ and $a(r)$ fix the variational parameters: f_1 and a_l ,

$$f(r) = 1 + \exp\left(-\frac{r}{\sqrt{2}\xi}\right) \sum_{l=0}^n (f_l r^l / l!), \tag{18}$$

$$a(r) = 1 + \exp\left(-\frac{r}{\lambda}\right) \sum_{l=0}^n (a_l r^l / l!). \tag{19}$$

To have single-value and finite functions for ψ and \mathbf{A} in the limit of $r \rightarrow 0$, we use $f = 0$ and $a^2 \rightarrow 0$. Note that in this method the G-L equations are not solved directly but by using their asymptotic behavior, we suggest some trial functions which minimize the free energy. The trial functions which minimize the free energy are solutions of the G-L equations, as well. For a vortex with vorticity two, asymptotic behavior gives to $f_1 = f_0 / \sqrt{2}\xi$ and all other coefficients are variational parameters which are determined numerically.

The G-L free energy of Eq. (37) is a function of fourth order with respect to variational parameters, called V_i in the following equation:

$$\begin{aligned} \mathcal{F} = & \mathcal{F}_0 + \sum_i \mathcal{F}_i^{(1)} V_i + \sum_{i \geq j} \mathcal{F}_{ij}^{(2)} V_i V_j \\ & + \sum_{i \geq j \geq k} \mathcal{F}_{ijk}^{(3)} V_i V_j V_k + \sum_{i \geq j \geq k \geq l} \mathcal{F}_{ijkl}^{(4)} V_i V_j V_k V_l. \end{aligned} \tag{20}$$

We recall that in our problem the variational parameters are f_i and a_i . The physical nature of the problem makes the surface $\mathcal{F}(f_i, a_i)$ concave and well behaved, so we use the Newton method of optimization [5, 13] with iteration procedure

$$V_i^{(m+1)} = V_i^{(m)} - \sum_j \left[\mathbf{H}^{-1} \right]_{ij} D_j^{(m)}, \tag{21}$$

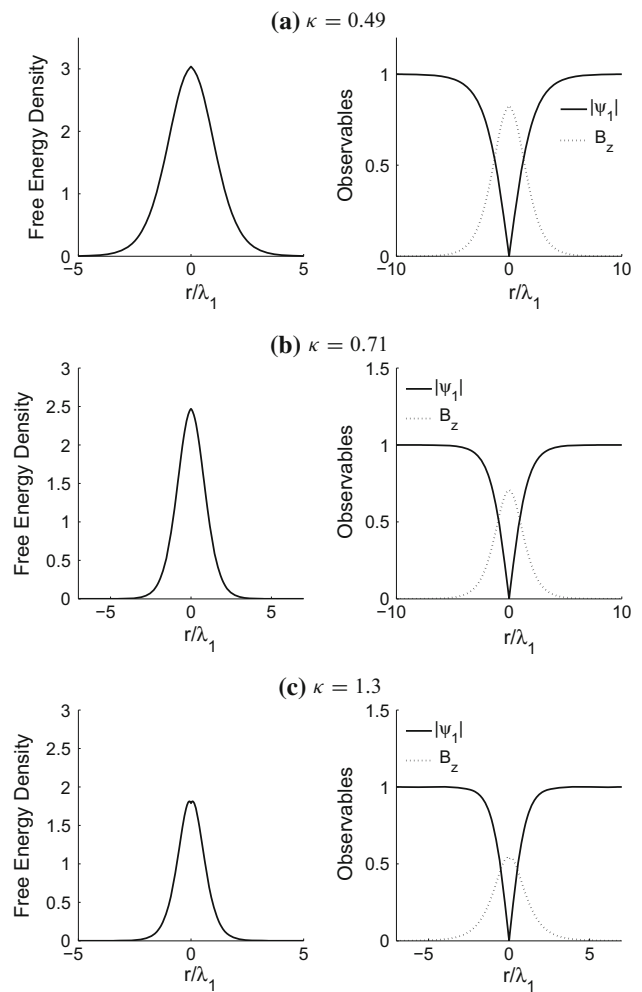


Fig. 1 Free energy density and condensation state and magnetic field profiles cross sections in a plane for three types of G-L parameter with winding number $n = 1$. $k = 0.49$ is for the type I superconductor. $k = 1.3$ is for the type II superconductor. The bulk behaviors of condensations and magnetic fields are the same for all three cases, as expected. Increasing the G-L parameter leads to a faster screening of the condensation and the magnetic field penetration depth decreases. The free energy value decreases by increasing the G-L parameter, as well

\mathbf{H} is the Hessian matrix and $D_i = \partial \mathcal{F} / \partial V_i |_{V_i = V_i^{(m)}}$. The stationary solution of this equation corresponds to the (local) minimum of the free energy. In our computations, changing initial values of V_i in the program does not change the obtained values of V_i , so the solutions correspond to the absolute minimum of the free energy. We use this method to obtain the variational parameters for vorticity one and two.

We use this variational method to calculate the variational parameters of the condensation states and magnetic field for three types of superconductors: type I for which $\xi = 51$ nm and $\lambda = 25$ nm and $\kappa < 1/\sqrt{2}$; type II for which $\xi = 19$ nm and $\lambda = 25$ nm and $\kappa > 1/\sqrt{2}$; the Bogomolny point where $\xi = 35$ nm, $\lambda = 25$ nm and $\kappa = 1/\sqrt{2}$. For these types of superconductors we use the variational parameters up to the

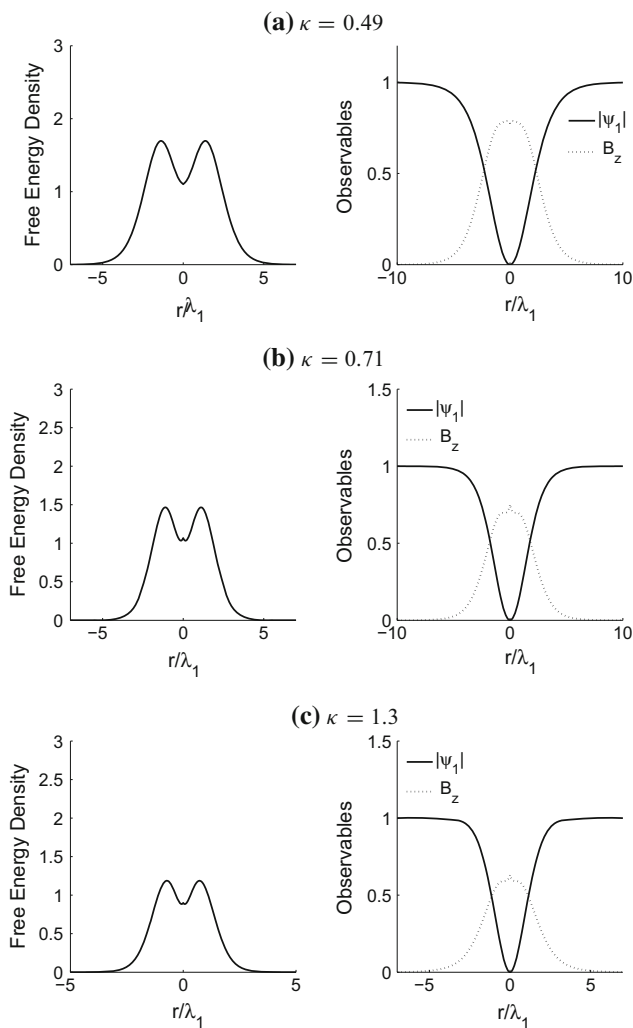


Fig. 2 Free energy density and condensation state and magnetic field profiles cross sections in a plane for the same G-L parameter as for Fig. 1a–c for winding number $n = 2$. The energy of a vortex formation decreases with increasing G-L parameter in the defined dimension of energy. Increasing the winding number to $n = 2$, the maximum of the free energy density leaves the origin core of the vortex to other values. The results of our program show the same behavior for the free energy density as in [3], which shows that by increasing the winding number, the maximum of the free energy density is located at further distances from the origin place of the core of the vortex

eighth polynomial terms. Using more terms and parameters does not change the free energy value up to the decimal point.

Figure 1 shows the condensation and magnetic field behaviors and also the free energy density for vorticity one for these three types. The free energies are 24.7, 4.8, and 12.3, respectively. Figure 2 shows the same functions for vorticity two for the same parameters of superconductor types of Fig. 1a–c. The free energies for winding number $n = 2$ are 42.9, 10.4, and 24.7, respectively. The dimension of energy is $E/(\alpha^2\lambda^2/\beta)$. The free energy of a system consisting of two vortices located far from each other is equal to the sum

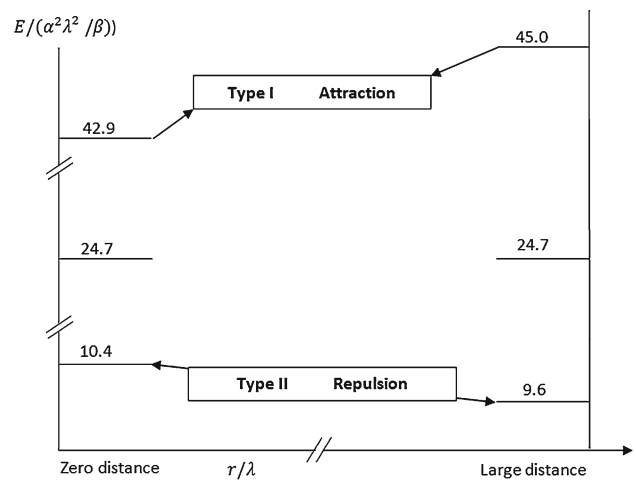


Fig. 3 Energy versus distance between two vortices of type I and II when they are far from each other and when they merge and form one giant vortex with winding $n = 2$, using the Rebbi variational method. For type I the energy of the giant vortex is smaller than two separate vortices, so the interaction is attraction. For type II the situation is reversed and the interaction is repulsion. For the case $\kappa = 1/\sqrt{2}$ there is no interaction between the vortices

of the free energy of two separate vortices with vorticity one. When they merge at zero distance, the energy is equal to the energy of a vortex with vorticity two. Therefore, if the energy of a vortex with vorticity two is larger than energy of two vortices with vorticity one, the interaction is repulsion and if the energy of a vortex with vorticity two is smaller than energy of two vortices with vorticity one, the interaction is attraction. Our results are 12.36828909 and 24.76771608 for $n = 1$ and $n = 2$, respectively, at the Bogomol’nyi point. For the Bogomol’nyi point there is no interaction, As $24.76771608 - 2 \times 12.36828909 = 0.0311379$ the meaningful number of our calculation is up to the decimal point in this dimension of energy. Our results for a system of two vortices are shown in Fig. 3, a repulsion for type II and an attraction for type I are observed and for $\kappa = 1/\sqrt{2}$ the vortices do not interact with each other. The results of [5] also show a monotonic type interaction type, attraction and repulsion between the vortices for type I and type II superconductors, respectively, at any arbitrary distances.

4 Interaction between the vortices in type 1.5 superconductor

In this case the magnetic penetration depth lies between the two correlation lengths. Therefore, the interaction type of attraction or repulsion is not clear by obtaining the asymptotic value of free energy. This is called the type 1.5 superconductor. Therefore, the variational method which has been used in the previous section must be applied considering details

for this type of superconductor to study the interactions for all distances. The free energy is of (3) type. For simplicity, it is assumed that the phase transition temperature is the same for both condensations. The G-L equations become

$$-\Psi_1 + |\Psi_1|^2\Psi_1 + \left(\frac{1}{i\kappa_1}\nabla - \mathbf{A}\right)^2\Psi_1 - \gamma\Psi_2 = 0, \quad (22)$$

$$-\frac{\alpha_2}{\alpha_1}\Psi_2 + \frac{\beta_2}{\beta_1}|\Psi_2|^2\Psi_2 + \frac{m_1}{m_2}\left(\frac{1}{i\kappa_1}\nabla - \mathbf{A}\right)^2\Psi_2 - \gamma\Psi_1 = 0, \quad (23)$$

$$\begin{aligned} \nabla \times \nabla \times \mathbf{A} = & \frac{1}{2i\kappa_1}(\Psi_1^*\nabla\Psi_1 - \Psi_1\nabla\Psi_1^*) - |\Psi_1|^2\mathbf{A} \\ & + \frac{m_1}{m_2}\left(\frac{1}{2i\kappa_1}(\Psi_2^*\nabla\Psi_2 - \Psi_2\nabla\Psi_2^*) - |\Psi_2|^2\mathbf{A}\right). \end{aligned} \quad (24)$$

Applying the London approximation to Eq. (24), one gets to an effective London penetration depth for the two-band superconductor:

$$\lambda = 1 / \left(\sqrt{|\Psi_{10}|^2 + \frac{m_1}{m_2}|\Psi_{20}|^2} \right). \quad (25)$$

For $\gamma > 0$, called positive coupling coefficient, the two condensates must have the same vorticity [13]. MgB_2 is an example of this kind of superconductors. λ is going to be used in the trial function of vector potential. When the winding numbers for the two condensations are not equal, the flux of the vortex is fractionally quantized and the energy diverges logarithmically [39]. These are not topologically stable structures. Throughout this article we do not consider these fractional vortices or a non-topological one. It is not possible to use the variational method for the situations when the phase or winding of all condensations are not equal.

Using the same vortex line ansatz as Sect. 3:

$$\Psi_i = f_i(r)e^{in\theta} \quad \text{and} \quad \mathbf{A} = \frac{na(r)}{\kappa_1 r}\mathbf{e}_\theta. \quad (26)$$

The G-L equations become

$$\begin{aligned} -f_1(r) + f_1^3(r) - \frac{1}{\kappa_1^2}\left(\partial_r^2 f_1 + \frac{1}{r}\partial_r f_1\right) \\ + \frac{n^2(a-1)^2}{\kappa_1^2 r^2} f_1 - \gamma f_2 = 0, \end{aligned} \quad (27)$$

$$\begin{aligned} -\frac{\alpha_2}{\alpha_1}f_2(r) + \frac{\beta_2}{\beta_1}f_2^3(r) \\ + \frac{m_1}{m_2}\left(-\frac{1}{\kappa_1^2}\left(\partial_r^2 f_2 + \frac{1}{r}\partial_r f_2\right) + \frac{n^2(a-1)^2}{\kappa_1^2 r^2}f_2\right) \\ - \gamma f_1 = 0, \end{aligned} \quad (28)$$

$$\partial_r a - \frac{1}{r}\partial_r a + \left(f_1^2 + \frac{m_1}{m_2}f_2^2\right)(1-a) = 0, \quad (29)$$

and for asymptotic behavior at $r \rightarrow \infty$

$$-1 + f_{10}^2 - \gamma\eta = 0, \quad (30)$$

$$-\frac{\alpha_2}{\alpha_1}\eta + \frac{\beta_2}{\beta_1}\eta^3(1 + \gamma\eta) - \gamma = 0, \quad (31)$$

f_{10} and f_{20} represent the behavior of the functions f_1 and f_2 at infinity. For simplicity $f_{20} = \eta f_{10}$, where η is a constant coefficient that relates two condensations to each other. To satisfy the boundary conditions at $r \rightarrow \infty$, one can choose the functions as follows:

$$f_1 = \sqrt{1 + \gamma\eta} + c_{f1} \exp\left(-\frac{r}{\sqrt{2}\xi_v}\right), \quad (32)$$

$$f_2 = \sqrt{\frac{\beta_1}{\beta_2}\left(\frac{\alpha_2}{\alpha_1} + \frac{\gamma}{\eta}\right)} + c_{f2} \exp\left(-\frac{r}{\sqrt{2}\xi_v}\right), \quad (33)$$

$$a = 1 + c_a \exp\left(-\frac{r}{\lambda_v}\right). \quad (34)$$

ξ_v is equivalent to the length scale of a small fluctuation in the bulk, and it is given by the largest solution to the equation

$$\begin{aligned} \left(2 + 3\gamma\eta - \frac{1}{2\kappa_1^2\xi_v^2}\right)\left(2\frac{\alpha_2}{\alpha_1} + 3\frac{\gamma}{\eta} - \frac{m_1}{m_2}\frac{1}{2\kappa_1^2\xi_v^2}\right) \\ - \gamma^2 = 0. \end{aligned} \quad (35)$$

Using Eqs. (26), (32) to (34) in Eq. (25), the penetration depth is

$$\lambda_v = 1 / \sqrt{\frac{m_1}{m_2}\frac{\beta_1}{\beta_2}\left(\frac{\alpha_2}{\alpha_1} + \frac{\gamma}{\eta}\right) + (1 + \gamma\eta)}. \quad (36)$$

Suggesting polynomial forms for c_{f1} , c_{f2} , and c_a , the trial functions are

$$f_1(r) = \sqrt{1 + \gamma\eta} + \exp\left(-\frac{r}{\sqrt{2}\xi_v}\right)\sum_{l=0}^n (f_{1,l}r^l/l!), \quad (37)$$

$$\begin{aligned} f_2(r) = \sqrt{\frac{\beta_1}{\beta_2}\left(\frac{\alpha_2}{\alpha_1} + \frac{\gamma}{\eta}\right)} \\ + \exp\left(-\frac{r}{\sqrt{2}\xi_v}\right)\sum_{l=0}^n (f_{2,l}r^l/l!), \end{aligned} \quad (38)$$

$$a(r) = 1 + \exp\left(-\frac{r}{\lambda_v}\right)\sum_{l=0}^n (a_l r^l/l!). \quad (39)$$

Boundary conditions determine some parameters and the remaining ones are variational parameters. Figure 4 shows the condensations and the magnetic field for a vortex with $\xi_1 = 51$ nm, $\xi_2 = 8$ nm and $\lambda_1 = 25$ nm, $\lambda_2 = 30$ nm parameters. Figure 5 shows the same fields for a vortex with vorticity two. The free energies are larger than the type I and II with the likely London penetration and condensation state. The energies of a vortex structures are 67.4 and 148.6 for winding numbers $n = 1$ and $n = 2$, respectively. The energy of formation of a stable vortex in these kinds of materials is larger than the one in type I and II.

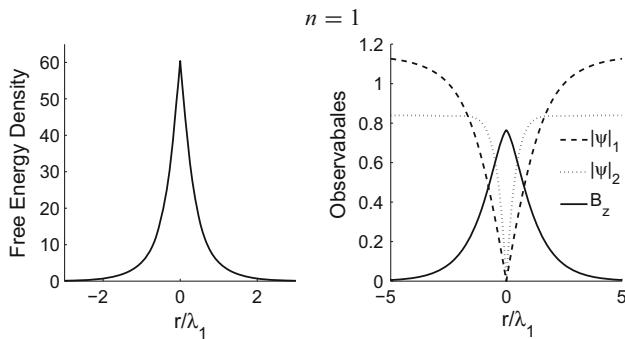


Fig. 4 Free energy density and condensations and magnetic field of a vortex in a type 1.5 superconductor with $\xi_1 = 51$ nm, $\xi_2 = 8$ nm and $\lambda_1 = 25$ nm, $\lambda_2 = 30$ nm with the winding number $n = 1$. The profile functions reach their asymptotic values at large distance

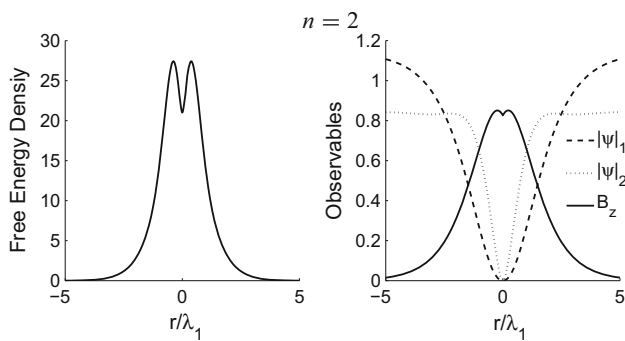


Fig. 5 Free energy density and condensations and magnetic field of a vortex in a type 1.5 superconductor with $\xi_1 = 51$ nm, $\xi_2 = 8$ nm, and $\lambda_1 = 25$ nm, $\lambda_2 = 30$ nm with the winding number $n = 2$. The energies of the vortex structure are 67.4 and 148.6 for winding numbers $n = 1$ and $n = 2$, respectively, in the defined unit of the free energy. The energy of the structure in this scale is larger than type I and II superconductors

So far we have obtained the trial functions for the condensation states and the magnetic field. Rebbi’s variational method is applied to obtain these solutions. We used this method for type I and II superconductors. Free energy values for $n = 1$ and $n = 2$ are obtained (Fig. 3). We have obtained the result that the free energy of a vortex with vorticity two is smaller than two vortices with $n = 1$ for type I, so the interaction in this type of superconductors is attraction. The free energy of a vortex with $n = 2$ is found to be larger than the free energy of two vortices with $n = 1$ in type II superconductors. The interaction between these vortices is repulsion.

Now we must apply the variational method to study the interaction of type 1.5 superconductors in which there is no monotonic interaction type for all range of distances. We must obtain the vortex profiles and magnetic field for all range of distances. To obtain trial functions of two vortices located at an arbitrary distance, Jacobs and Rebbi used conformal transformation of the complex plane z . z is defined as $z = x + iy$. With this transformation [5], we have two image

vortex profiles centered at $\pm d/2$ in z' plane instead of zero in z plane. For a phase change of 2π in z' plane there is a phase change of 4π in the z plane, so this is a map of one vortex to two vortices profiles. The wave function in the complex plane can be defined as

$$\Psi_i(z, z^*) = \left\{ \left[z^2 - \left(\frac{d}{2}\right)^2 \right] / \left[z^{*2} - \left(\frac{d}{2}\right)^2 \right] \right\}^{1/2} \times f_i(z, z^*). \tag{40}$$

For our calculation we consider the case with equal vorticity of all the condensations. We use this projection between two polar coordinates which is different from the Jacobs coordinate system. With this projection or mathematical trick, one can use the trial function of one vortex to obtain the trial function of two vortices in another plane called “ r' -plane”. Then it is possible to calculate the interaction between the vortices in this projected plane. The coordinate system of the vortices in r' -plane is defined by $r = r'^2 - (d/2)^2$ and $\theta' = 2\theta$. $\pm d/2$ represents the locations of the two vortices. The trial function f_i should describe not only the interaction between two separate vortices but also the solution of a giant vortex with vorticity two for the case when they merge [5, 13]. Two vortices are independent when $d \rightarrow \infty$, while at $d \sim 0$ they merge and form one giant vortex with vorticity two. In addition, we also need another term to describe the interaction between two vortices. Therefore, the trial function can be constructed as

$$f_i(r, \theta) = \omega f_i^{(1)} \left(\left| r - \frac{d}{2} \right| \right) f_i^{(1)} \left(\left| r + \frac{d}{2} \right| \right) + (1 - \omega) \frac{\left| r^2 - \left(\frac{d}{2}\right)^2 \right|}{|r^2|} f_i^{(2)}(|r|) + \delta f_i(r, \theta), \tag{41}$$

δf_i accounts for the interaction and $f_i^{(1)}$ and $f_i^{(2)}$ are single-vortex solutions with vorticity one and two, respectively, and they are obtained by the method introduced for a single vortex. ω interpolates between two independent vortices and one giant-vortex solutions. The factor in the second term at the right-hand-side of Eq. (41) ensures that the wave function vanishes at the vortex cores $r = \pm d/2$. The interaction contribution may be constructed as follows:

$$\delta f_i(r, \theta) = \left| r^2 - \left(\frac{d}{2}\right)^2 \right| \frac{1}{\cosh(\sqrt{2}\kappa_1|r|)} \times \sum_{l=0}^n \sum_{j=0}^l f_{i,l,j} \frac{|r|^{2l}}{2} \left[(e^{2i\theta})^j + (e^{-2i\theta})^j \right]. \tag{42}$$

The first factor is to make sure that the wave function vanishes at the vortex cores, and the second factor accounts for the fact that the interaction vanishes when $r \rightarrow \infty$. I

in the exponentials represents $i = \sqrt{-1}$, which is typed in capital form to avoid any confusion with the “i” in the summation. When we put two vortices in a plane, the circular symmetry would be lost. Only a reflection symmetry with respect to the plane would remain. The polynomial in the above equation preserves such a reflection symmetry.

The same procedure which is applied to f_i for constructing ψ_i applies to \mathbf{A} :

$$\begin{aligned} \mathbf{A} = \omega & \left[\frac{1}{\kappa_1 |r - d/2|} a^{(1)} \left(\left| r - \frac{d}{2} \right| \right) \right. \\ & \left. + \frac{1}{\kappa_1 |r + d/2|} a^{(1)} \left(\left| r + \frac{d}{2} \right| \right) \right] \\ & + \frac{2}{\kappa_1 r} (1 - \omega) a^{(2)}(|r|) + \delta a(r, \theta), \end{aligned} \tag{43}$$

where $a^{(1)}$ and $a^{(2)}$ are functions of the single-vortex solutions with vorticities one and two. The asymptotic behavior of vortices implies the interaction contribution and it has the following form:

$$\delta a(r, \theta) = \frac{1}{\cosh(|r|)} [ra_1(r, \theta) + ra_2(r, \theta)], \tag{44}$$

with

$$a_k(r, \theta) = \sum_{i=0}^n \sum_{j=0}^i a_{k,ij} \frac{|r|^{2i}}{2} \left[\left(e^{(2I\theta)} \right)^j + \left(e^{(-2I\theta)} \right)^j \right], \tag{45}$$

where $k = 1, 2$. $f_{i,l,j}$ and $a_{k,ij}$ are new variational parameters which must be obtained numerically. We consider the variational parameters up to the coefficients of $|r|^6$ in our calculations.

Figure 6 shows the condensation states, magnetic fields, and free energy density between two type 1.5 vortices at different distances. Figures 5 and 6 shows that by increasing d the distribution of the magnetic field changes such that for large d , each vortex has its own magnetic field, almost independently. However, as $d \rightarrow 0$, the magnetic field is distributed along the vortex with vorticity two, as expected. In Fig. 7 we show a three dimensional magnetic field of two vortices at the distance $d = 2$. Only the so-called reflection symmetry remains. Figure 8 shows the interaction energy versus distance between two vortices. As the distance between the vortices decreases the energy decreases up to distance 2.7, so the interaction between two vortices in this range of distances is attraction. The energy increases from distance 2.7 to zero, so the interaction is repulsion. Our results agree with the results obtained in Ref. [13]. We also obtain the same stability point by choosing the same penetration depth and correlation length, but with other different parameters such as γ . In addition, we use the polar coordinate system instead of a Cartesian coordinate system. The polar coordinate system simplifies calculations when we have only a vortex in

the plane with circular symmetry. When two vortices are imposed in a plane, this circular symmetry is lost and only a reflection symmetry with respect to the plane at the middle of the distance from the centers of the vortices survives. Because of losing the circular symmetry, the θ dependence of the functions is included again (Fig. 7).

5 Interaction between the vortices with three condensation states

What about the situation with three condensation states? The idea of a vortex with three condensation states can be used to describe the iron-based superconductors. Also, Babaev and Weston have recently studied the possibility of the existence of more than three condensation states from a theoretical point of view [21]. We use the method of previous section for a case with three condensations. For simplicity, we study the cases for which the interband scattering couplings are equal. The equations of motions are obtained by using (6) for the G-L free energy for the three states,

$$-\Psi_1 + |\Psi_1|^2 \Psi_1 + \left(\frac{1}{i\kappa_1} \nabla - \mathbf{A} \right)^2 \Psi_1 - \gamma \Psi_2 - \gamma \Psi_3 = 0, \tag{46}$$

$$\begin{aligned} -\frac{\alpha_2}{\alpha_1} \Psi_2 + \frac{\beta_2}{\beta_1} |\Psi_2|^2 \Psi_2 + \frac{m_1}{m_2} \left(\frac{1}{i\kappa_1} \nabla - \mathbf{A} \right)^2 \Psi_2 \\ - \gamma \Psi_1 - \gamma \Psi_3 = 0, \end{aligned} \tag{47}$$

$$\begin{aligned} -\frac{\alpha_3}{\alpha_1} \Psi_3 + \frac{\beta_3}{\beta_1} |\Psi_3|^2 \Psi_3 + \frac{m_1}{m_3} \left(\frac{1}{i\kappa_1} \nabla - \mathbf{A} \right)^2 \Psi_3 \\ - \gamma \Psi_1 - \gamma \Psi_2 = 0, \end{aligned} \tag{48}$$

$$\begin{aligned} \nabla \times \nabla \times \mathbf{A} = \frac{1}{2i\kappa_1} (\Psi_1^* \nabla \Psi_1 - \Psi_1 \nabla \Psi_1^*) - |\Psi_1|^2 \mathbf{A} \\ + \frac{m_1}{m_2} \left(\frac{1}{2i\kappa_1} (\Psi_2^* \nabla \Psi_2 - \Psi_2 \nabla \Psi_2^*) - |\Psi_2|^2 \mathbf{A} \right) \\ + \frac{m_1}{m_3} \left(\frac{1}{2i\kappa_1} (\Psi_3^* \nabla \Psi_3 - \Psi_3 \nabla \Psi_3^*) - |\Psi_3|^2 \mathbf{A} \right). \end{aligned} \tag{49}$$

As mentioned above, $\gamma_1 = \gamma_2 = \gamma_3$, which means that the strength of all interband couplings are equal. Equation (49) describes the screening of the magnetic field by the superconducting condensates. Again, using the London approximation, the effective London penetration depth for three-band superconductors is

$$\lambda_v = 1 / \sqrt{|\Psi_{10}|^2 + \frac{m_1}{m_2} |\Psi_{20}|^2 + \frac{m_1}{m_3} |\Psi_{30}|^2}, \tag{50}$$

where Ψ_{i0} is the bulk value of the i th superconducting condensate. Since all the response of three-band superconductors to the magnetic fields is described by a single length scale λ , all condensates couple to the same gauge field. The interband coupling changes the bulk value, and it modifies

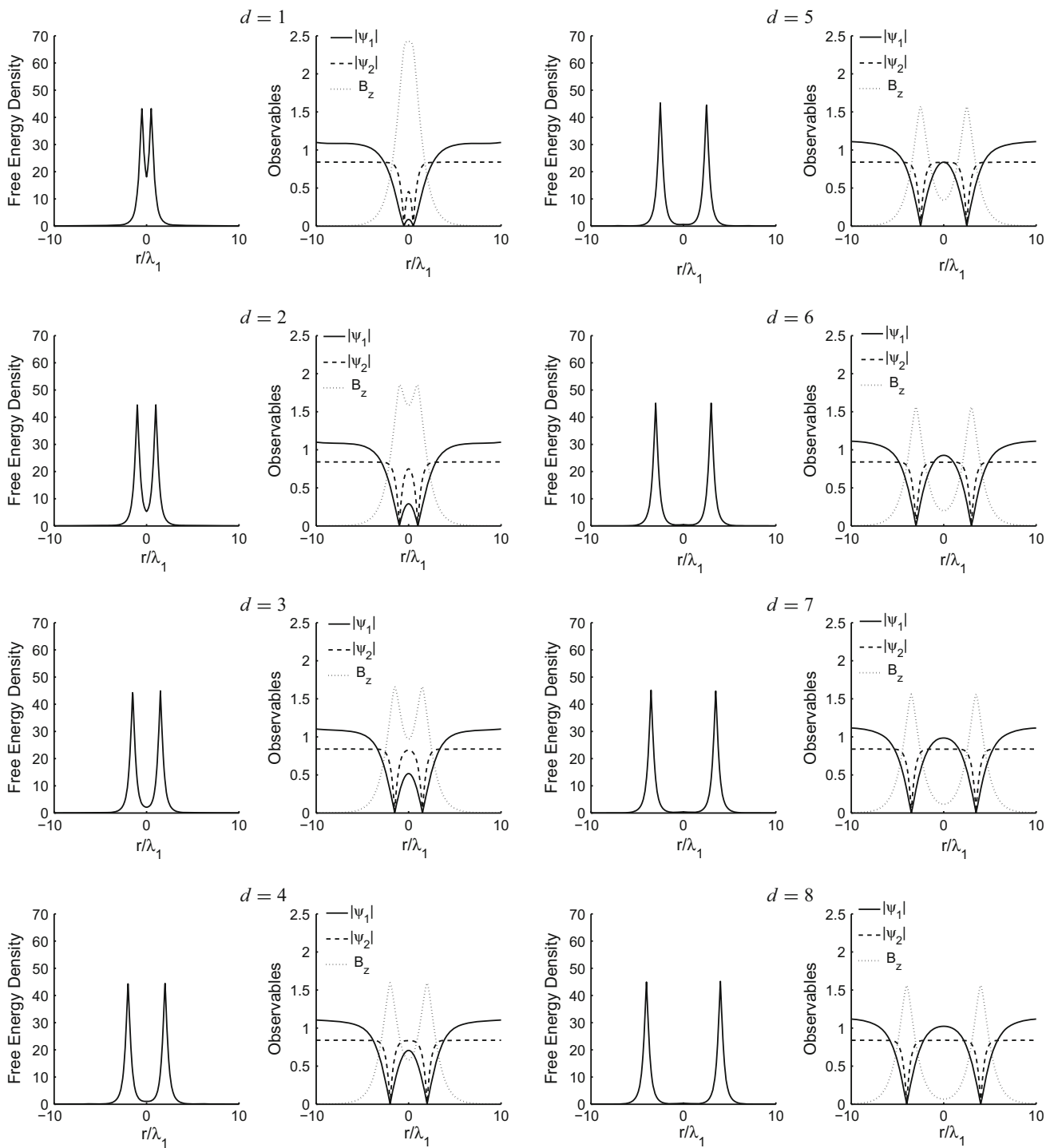


Fig. 6 Free energy density, condensation states, and magnetic field profiles cross sections in a plane when two vortices of type 1.5 are located at different distances. As the separation between the vortices

increases the magnetic field profile decreases between the vortices. When the vortices are far from each other they are like two separate vortices with no interaction

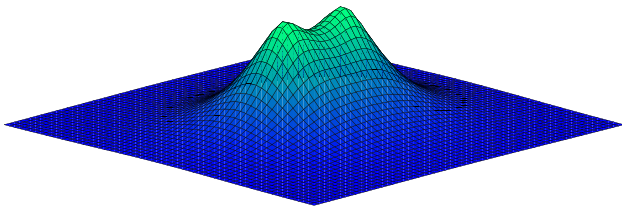


Fig. 7 A three dimensional plot of the magnetic field of two vortices of type 1.5 at distance $d = 2$. No circular symmetry is present any more. Only a reflection symmetry with respect to the plane at the middle distance between the vortices is present

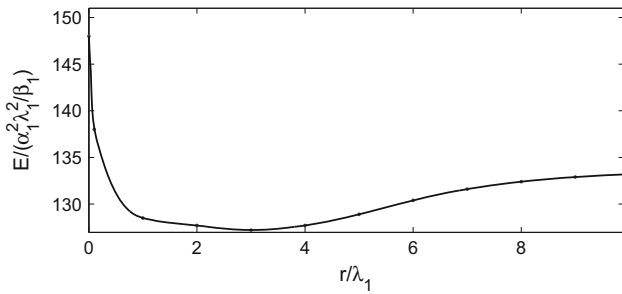


Fig. 8 Energy of two vortices of type 1.5, located at different distances. This shows a stability point at 2.7. At larger distance than 2.7 this energy increases, so at these separations the interaction is attraction. At smaller distances than 2.7, the energy increases and leads to repulsion between the vortices

the corresponding penetration depth. Again, we use the so-called ansatz (10) and obtain the equations

$$-f_1(r) + f_1^3(r) - \frac{1}{\kappa_1^2} \left(\partial_r^2 f_1 + \frac{1}{r} \partial_r f_1 \right) + \frac{n^2(a-1)^2}{\kappa_1^2 r^2} f_1 - \gamma f_2 - \gamma f_3 = 0, \tag{51}$$

$$-\frac{\alpha_2}{\alpha_1} f_2(r) + \frac{\beta_2}{\beta_1} f_2^3(r) + \frac{m_1}{m_2} \times \left(-\frac{1}{\kappa_1^2} \left(\partial_r^2 f_2 + \frac{1}{r} \partial_r f_2 \right) + \frac{n^2(a-1)^2}{\kappa_1^2 r^2} f_2 \right) - \gamma f_1 - \gamma f_3 = 0, \tag{52}$$

$$-\frac{\alpha_3}{\alpha_1} f_3(r) + \frac{\beta_3}{\beta_1} f_3^3(r) + \frac{m_1}{m_3} \left(-\frac{1}{\kappa_1^2} \left(\partial_r^2 f_2 + \frac{1}{r} \partial_r f_3 \right) + \frac{n^2(a-1)^2}{\kappa_1^2 r^2} f_3 \right) - \gamma f_1 - \gamma f_2 = 0, \tag{53}$$

$$\partial_r^2 a - \frac{1}{r} \partial_r a + \left(f_1^2 + \frac{m_1}{m_2} f_2^2 + \frac{m_1}{m_3} f_3^2 \right) (1-a) = 0. \tag{54}$$

In the limit when $r \rightarrow \infty$, the wave functions are defined by the bulk values f_{10} , f_{20} , and f_{30} . Defining $f_{20} = \eta f_{10}$ with $\eta > 0$ and $f_{30} = \eta' f_{10}$ with $\eta' > 0$, we have the equations for f_{10} , η , and η' :

$$-1 + f_{10}^2 - \gamma \eta - \gamma \eta' = 0, \tag{55}$$

$$-\frac{\alpha_2}{\alpha_1} \eta + \frac{\beta_2}{\beta_1} \eta^3 (1 + \gamma \eta + \gamma \eta') - 2\gamma = 0, \tag{56}$$

$$-\frac{\alpha_3}{\alpha_1} \eta' + \frac{\beta_3}{\beta_1} \eta'^3 (1 + \gamma \eta + \gamma \eta') - 2\gamma = 0. \tag{57}$$

The radial variation of the wave functions and the vector potential in the asymptotic region for $r \rightarrow \infty$ is found and is given by

$$f_1 = \sqrt{1 + \gamma \eta + \gamma \eta'} + c_{f1} \exp\left(-\frac{r}{\sqrt{2}\xi_v}\right), \tag{58}$$

$$f_2 = \sqrt{\frac{\beta_1}{\beta_2} \left(\frac{\alpha_2}{\alpha_1} + \frac{\gamma + \gamma'}{\eta + \eta'} \right)} + c_{f2} \exp\left(-\frac{r}{\sqrt{2}\xi_v}\right), \tag{59}$$

$$f_3 = \sqrt{\frac{\beta_1}{\beta_3} \left(\frac{\alpha_3}{\alpha_1} + \frac{\gamma + \gamma'}{\eta + \eta'} \right)} + c_{f3} \exp\left(-\frac{r}{\sqrt{2}\xi_v}\right), \tag{60}$$

$$a = 1 + c_a \exp\left(-\frac{r}{\lambda_v}\right). \tag{61}$$

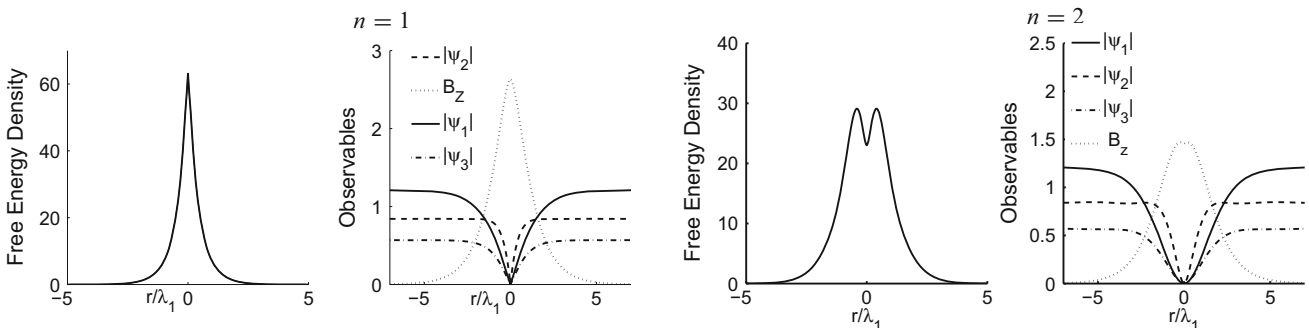


Fig. 9 Free energy density and condensations and magnetic field of a vortex with three condensation states with $\xi_1 = 51$ nm, $\xi_2 = 8$ nm, $\xi_3 = 25$ nm, and $\lambda_1 = 25$ nm, $\lambda_2 = 30$ nm, $\lambda_3 = 51$ nm, using the variational method, but a polar coordinate system is used. The energy of the

vortex is 85.2 for $n = 1$ and 189.5 for $n = 2$ in the defined dimension unit. The energy of the structure in this scale is larger than type I and II superconductors

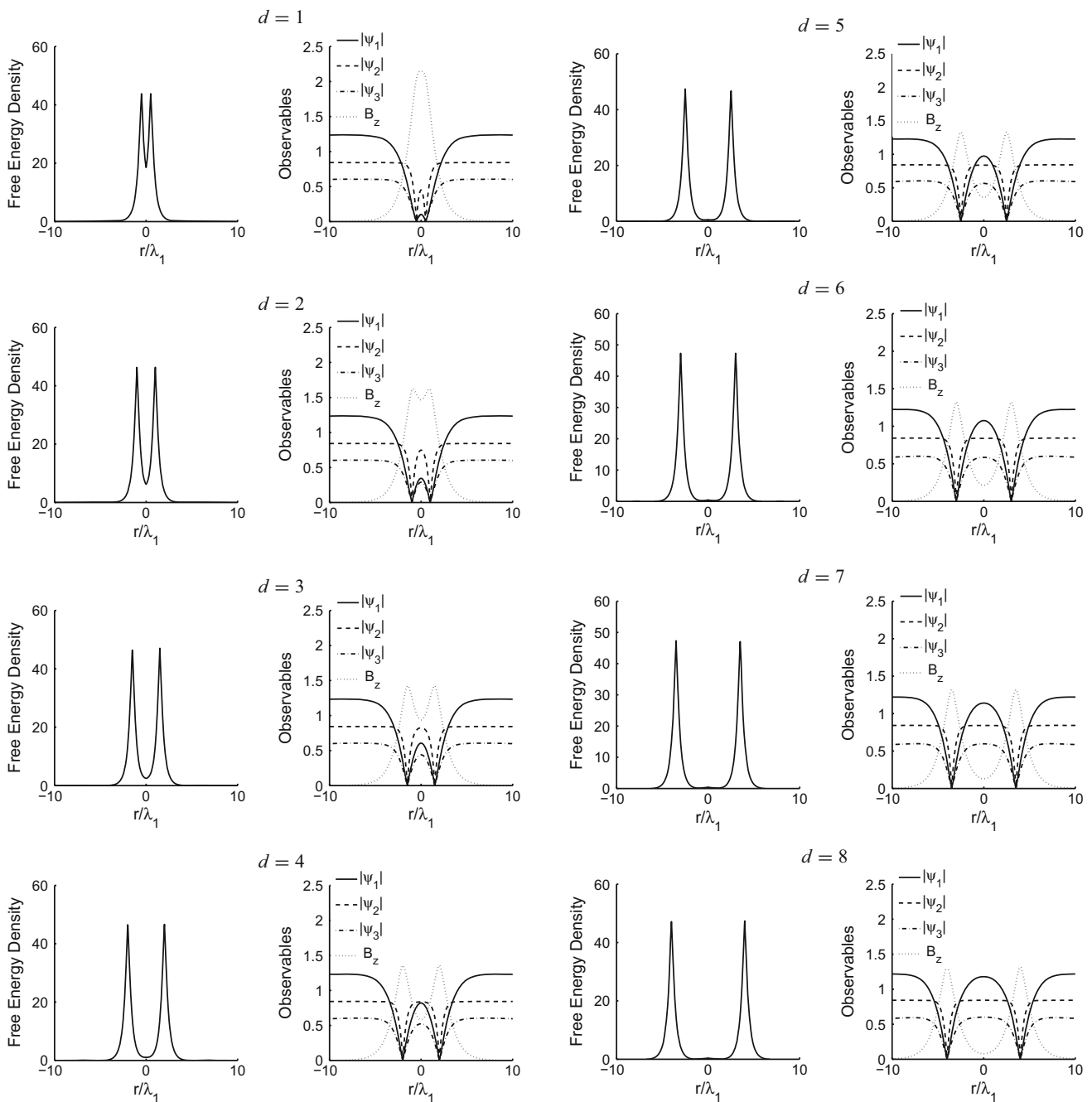


Fig. 10 Free energy density and condensation states and magnetic field profiles cross sections in a plane for two vortices with three condensations at different distances using the variational method. As the distance increases, the magnetic field profile function decreases between the vortices. When the vortices are close to each other the magnetic field profile function shows an increase. Repulsion between the vortices happens as

a result of the increase of the magnetic field. A change of the behavior of the first condensation relative to the other condensations from the distance $d = 1$ up to the distance $d = 4$ is observed. This shows that the rate of change of energy versus the distance between two vortices at such distances is not monotonic

At large distances, there is only one length scale for the three condensates, called the penetration depth λ_v . It can be obtained straightforwardly from Eqs. (58), (59), (60), and (50):

$$\lambda_v = 1 / \sqrt{\sum_{p=2,3} \frac{m_1 \beta_1}{m_p \beta_p} \left(\frac{\alpha_p}{\alpha_1} + \frac{\gamma + \gamma'}{\eta + \eta'} \right) + (1 + \gamma\eta + \gamma\eta')}. \tag{62}$$

To calculate the correlation length, we substitute the asymptotic limits of Eqs. (58) to (61) into Eqs. (49) to (53) and linearize the equations by considering only the linear parts of the terms. The following equation is obtained as a result of these procedures:

$$\left(2 + 3\gamma\eta - \frac{1}{2\kappa_1^2\xi_v^2}\right) \left(2\frac{\alpha_2}{\alpha_1} + 3\frac{\gamma}{\eta} - \frac{m_1}{m_2} \frac{1}{2\kappa_1^2\xi_v^2}\right) \times \left(2\frac{\alpha_3}{\alpha_1} + 3\frac{\gamma'}{\eta'} - \frac{m_1}{m_3} \frac{1}{2\kappa_1^2\xi_v^2}\right) - \gamma^3 = 0. \tag{63}$$

ξ_v is equivalent to the length scale of the small fluctuations in the bulk and is given by the largest solution to the equation. ξ_v is an effective length which is in fact the correlation in a system with interband coupling. With this new definition, the trial functions become

$$f_1(r) = \sqrt{1 + 2\gamma\eta} + \exp\left(-\frac{r}{\sqrt{2}\xi_v}\right) \sum_{l=0}^n (f_{1,l}r^l/l!), \tag{64}$$

$$f_2(r) = \sqrt{\frac{\beta_1}{\beta_2} \left(\frac{\alpha_2}{\alpha_1} + \frac{\gamma}{\eta}\right)} + \exp\left(-\frac{r}{\sqrt{2}\xi_v}\right) \sum_{l=0}^n (f_{2,l}r^l/l!), \tag{65}$$

$$f_3(r) = \sqrt{\frac{\beta_1}{\beta_3} \left(\frac{\alpha_3}{\alpha_1} + \frac{\gamma}{\eta}\right)} + \exp\left(-\frac{r}{\sqrt{2}\xi_v}\right) \sum_{l=0}^n (f_{3,l}r^l/l!), \tag{66}$$

$$a(r) = 1 + \exp\left(-\frac{r}{\lambda_v}\right) \sum_{l=0}^n (a_l r^l/l!), \tag{67}$$

where $f_{1,l}$, $f_{2,l}$, $f_{3,l}$, and a_l are variational parameters. Following the procedure of the previous sections, we obtain the variational coefficients, from which we can obtain the vortex solution. We truncate the higher-order corrections of the trial functions at $n = 6$ and find the solution of a single vortex with vorticity one and two. The penetration depths and correlation lengths we consider for our calculation are $\xi_1 = 51$ nm, $\xi_2 = 8$ nm, $\xi_3 = 25$ nm and $\lambda_1 = 25$ nm, $\lambda_2 = 30$ nm, $\lambda_3 = 51$ nm. We take $\gamma = \gamma' = 0.4 > 0$ and also $\eta = \eta' = 0.5$ for our calculation.

We plot the free energy and the functions profiles in Fig. 9. The energy of the vortex is 85.2 for $n = 1$ and 189.5 for $n = 2$. We can see the role of increasing the number of condensations in increasing the energy of formation of a vortex in these materials. The phenomenon has been observed when we had two condensations compared with the case when we had one condensation.

We plot the energy versus distance by the same method as the previous section. Figure 10 shows the free energy density and vortex profiles of two vortices at different distances. Figure 11 shows the free energy of two vortices versus distances. Again there is a repulsion between two vortices at short distances and attraction when they are far from each

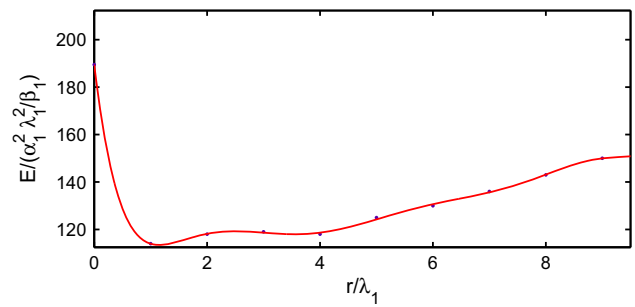


Fig. 11 Interaction energy dependence on distance between two vortices with three condensation states obtained by the variational method. There are two stability points at distances 1 and 4. At large distances there is attraction between these vortices. At small distances the interaction is repulsion. Two stability points lead to more complex structure for the location of vortices in these materials. Also it may have some novel practical usage

other. There are two stability points for these vortices, one in 4 and the other at 1. So, three condensations states can be different with respect to the two condensation states: the number of stability points is increased and the energy of the vortex formation increases compared with the superconductors of type I and II and 1.5. Note that the presence of two stable points depends on the value of the parameters of the model. One could consider the correlation lengths and penetration depths relative to each other such that it leads to only one stable point.

Because of the existence of two stability points, quantum tunneling may occur for the system of two vortices between the two stability points if one considers the time in the calculations. This may lead to the possibility of the existence of another topological structure, such as an instanton, in the superconductor materials with three condensation states. The possibility of the existence of Skyrme structures in these materials has recently been studied theoretically [40]. This evidence suggests that the Ginzburg–Landau Lagrangian with three condensations has theoretical properties which do not have an analog in the ordinary superconductors.

6 Conclusion

We use a numerical method to obtain the vortex profiles and the interaction between the vortices for a three condensation state superconductor. In this method, we use some trial functions for condensations and the magnetic field. The variational parameters of these functions are obtained by minimizing the free energy. We calculate the free energy density integral which is the energy of vortex formation in a polar coordinate system. The energy of a vortex with three condensations is higher than the two condensation states. The energy of two condensations is also larger than for type I and II super-

conductors with the same penetration depth and correlation length. Since these materials with two and three condensations are high temperature superconductors, it might be a hint that there is a relation between the energy of this structure and the higher phase transition temperature [41] in this type of superconductor. We have figured out that there are different types of interactions between these vortices: In type I and II superconductors, the interaction energy of a vortex with winding $n = 2$ and two vortices with $n = 1$ can show the type of interaction when they are far from each other. We have obtained attraction for type I and repulsion for type II superconductors. Using a full procedure of the variational method for a type 1.5 superconductor in a polar coordinate system, we obtain repulsion at smaller distances than $2.7/\lambda_1$ and attraction at larger distances. There is a stability point for vortices at $2.7\lambda_1$ in this case. For three condensations, we have seen the same behavior as the two condensations; but there are two stability points at 4 and 1.

Currents and magnetic fields lead to a repulsion type of interaction and also the core of the condensation can lead to an attraction type of interaction when $r \gg 1$ [31,32]. For type I where $\frac{\lambda}{\xi} < \frac{1}{\sqrt{2}}$, the core of the magnetic field is smaller than the core of the condensation. Thus, the winner of the interaction is attraction [4, 14–20]. For type II the situation is reversed and a repulsion interaction exists. A type 1.5 superconductor with $\xi_1 \ll \lambda_1$ and $\lambda_2 \ll \xi_2$ can be considered as superconductor of type II according to the ξ_1 , λ_1 and a superconductor of type I according to ξ_2 , λ_2 . The size of the core of one of the components is the largest length scale of the problem. Therefore a region domination of the repulsive interaction mediated by currents and magnetic field and a region of domination of the attraction mediated by the largest length scale of the problem exist. A schematic view of this type of superconductor is illustrated in [31,32]. The stability point is at the border of these two regions. A superconductor with three condensations with $\xi_1 \gg \lambda_1$, $\lambda_2 \gg \xi_2$, and $\lambda_3 \gg \xi_3$ can be considered as two type 1.5 superconductors. $\xi_1 \gg \lambda_1$ and $\lambda_2 \gg \xi_2$ represent a superconductor of type 1.5 with a stability point at $2.7\lambda_1$. $\xi_1 \gg \lambda_1$ and $\lambda_3 \gg \xi_3$ represents another type 1.5 with a stability point at another location. When all of these length scales are present there is competition between these two type 1.5 superconductors. This may lead to the existence of two stability points. There exists an effective penetration depth for large distances. This length is obtained from the London approximation. The effective penetration length will be important when the gradients of the condensations are negligible. This happens when r is in the region where all the condensations obtain their asymptotic values. However, the situation is different for smaller distances. Three individual penetration depths are introduced because of the response of the magnetic field to each condensation. The competition between repulsion given by penetration depths and attractive mechanisms given by conden-

sations changes the monotonic behavior of the energy for three condensation superconductors, especially for intermediate distances (Fig. 11). However, the interband coupling and the nonlinearity of the equations make the system more complex than the above simple description. So the number of stable points depends on the values of these three correlation lengths and penetration depths of the model. Here we use a penetration depth which conveys all other lengths of the model. One could use parameters that do not lead to such a system with two stable point. The existence of two stable points may have novel applications. Because of the existence of two stability points, quantum tunneling may occur for the system of two vortices between the two stability points if one considers the time in the calculations. This may lead to the possibility of the existence of another topological structure, such as the instanton, in the superconductor materials with three condensation states. The possibility of the existence of Skyrme structures in these materials has recently been studied theoretically [40]. Recent experimental observation on the vortex behavior in these type of materials, which can be described with three condensations, have been shown to have different behavior of the vortices [42,43]. This evidence suggests that the Ginzburg–Landau Lagrangian with three condensations has theoretical properties which do not have an analog in ordinary superconductors. If the energy of these structures has something to do with the temperature, then theoretically we can predict what values of the correlation lengths and penetration depths lead to a higher energy for the vortex formation and therefore a higher phase transition temperature. If, seen from the experimental point of view, making or finding such materials with these penetration depths and correlation lengths is made possible, higher critical temperature than the current ones can be reachable. It may be possible to apply this numerical method to study the interaction between special types of non-abelian vortices.

Acknowledgments We are grateful to the research council of the University of Tehran for supporting this study.

Open Access This article is distributed under the terms of the Creative Commons Attribution License which permits any use, distribution, and reproduction in any medium, provided the original author(s) and the source are credited.

Funded by SCOAP³ / License Version CC BY 4.0.

References

1. H. Yukawa, PTP **17**, 48 (1935)
2. M. Eto, Y. Hirono, M. Nitta, S. Yasui, PTEP **01**, 012 (2014)
3. N. Manton, S. Sutcliffe, *Topological Solitons* (Cambridge University Press, New York, 2004)
4. L. Kramer, Phys. Rev. B **3**, 3821 (1971)
5. L. Jacobs, C. Rebbi, Phys. Rev. B **19**, 4486 (1979)
6. L. Ginzburg, L.D. Landau, Zh. Eksp. Teor. Fiz. **20**, 1046 (1950)

7. N. Tinkham, *Introduction to Superconductivity* (McGraw-Hill Inc., New York, 1996)
8. A. Abrikosov, Zh. Eksp. Teor. Fiz. **32**, 1442 (1957)
9. H.B. Nielsen, P. Olesen, Nucl. Phys. B **61**, 45 (1973)
10. H.B. Nielsen, P. Olesen, Nucl. Phys. B **160**, 380 (1979)
11. J. Ambjørn, P. Olesen, Nucl. Phys. B **170**, 265 (1980)
12. J.N. Annett, *Superconductivity, Superfluids, and Condensates* (Oxford University Press, New York, 2004)
13. S.Z. Lin, X. Hu, Phys. Rev. B **84**, 214505 (2011)
14. A. Chaves, F.M. Peeters, G.A. Farias, M.V. Milosevic, Phys. Rev. B **83**, 054516 (2011)
15. E.H. Brandt, Phys. Rev. B **34**, 6514 (1986)
16. J.M. Speight, Phys. Rev. D **55**, 3830 (1997)
17. R. MacKenzie, M.-A. Vachon, U.F. Wichoski, Phys. Rev. D **67**, 105024 (2003)
18. L.M.A. Bettencourt, R.J. Rivers, Phys. Rev. D **51**, 1842 (1995)
19. F. Mohamed, M. Troyer, G. Blatter, I. Luk'yanchuk, Phys. Rev. B **65**, 224504 (2002)
20. A.D. Hernandez, A. Lopez, Phys. Rev. B **77**, 144506 (2008)
21. D. Weston, E. Babaev, Phys. Rev. B **88**, 214507 (2013)
22. J. Nagamatsu, N. Nakagawa, T. Muranaka, Y. Zenitani, J. Akimitsu, Nature **410**, 63 (2001)
23. Y. Kamihara, T. Watanabe, M. Hosono, J. Am. Chem. Soc. **130**, 3296 (2008)
24. Y. Tanaka, Phys. Rev. Lett. **88**, 017002 (2001)
25. E. Babaev, Phys. Rev. Lett. **89**, 067001 (2002)
26. E. Babaev, J. Jaykka, M. Speight, Phys. Rev. Lett. **103**, 237002 (2009)
27. L.F. Chibotaru, V.H. Dao, Phys. Rev. B **81**, 020502 (2010)
28. R. Geurts, M.V. Milosevic, F.M. Peeters, Phys. Rev. B **81**, 214514 (2010)
29. G. Blumberg, A. Mialitsin, B.S. Dennis, M.V. Klein, N.D. Zhigadlo, J. Karpinski, Phys. Rev. Lett. **99**, 227002 (2007)
30. X.X. Xi, Rep. Prog. Phys. **71**, 116501 (2008)
31. E. Babaev, M. Speight, Phys. Rev. B **72**, 180502 (2005)
32. E. Babaev, J. Carlstrom, M. Speight, Phys. Rev. Lett. **105**, 067003 (2010)
33. M. Faber, J. Greensite, S. Olejnik, Phys. Rev. D **57**, 2603 (1998)
34. S. Deldar, Phys. Rev. D **62**, 034509 (2000)
35. S. Deldar, S. Rafibakhsh, Phys. Rev. D **76**, 094508 (2007)
36. J. Greensite, K. Langfeld, S. Olejnik, H. Reinhardt, T. Tok, Phys. Rev. D **75**, 034501 (2007)
37. S. Deldar, S. Rafibakhsh, Phys. Rev. D **81**, 054501 (2010)
38. S. Deldar, H. Lookzadeh, S.M. Hosseini Nejad, Phys. Rev. D **85**, 054501 (2012)
39. E. Babaev, N.W. Ashcroft, Nat. Phys. **3**, 530 (2007)
40. J. Garaud, K.A.H. Sellin, J. Jaykka, E. Babaev, Phys. Rev. B **89**, 104508 (2014)
41. H. Klienert, *Gauge Fields in Condensed Matter* (World Scientific, Singapore, 1990)
42. P.J.W. Moll, L. Balicas, V. Geshkenbein, G. Blatter, J. Karpinski, N.D. Zhigadlo, B. Batlogg, Nat. Mater. **12**, 134 (2013)
43. P.J.W. Moll, L. Balicas, V. Geshkenbein, G. Blatter, J. Karpinski, N.D. Zhigadlo, B. Batlogg, Nat. Phys. (accepted). [arXiv:1405.5693](https://arxiv.org/abs/1405.5693)